applied optics

JPEG Pleno holography presents the numerical reconstruction software for holograms: an excursion in holographic views

Tobias Birnbaum,[1,2,*] Raees K. Muhammad,[1,2] Cristian Perra,[3] Antonin Gilles,[4] David Blinder,[1,2] Tomasz Kozacki,[5] and Peter Schelkens[1,2]

[1]Department of Electronics and Informatics (ETRO), Vrije Universiteit Brussel (VUB), Brussels, Belgium
[2]imec, Kapeldreef 75, B-3001 Leuven, Belgium
[3]Department of Electrical and Electronic Engineering, CNIT Research Unit, University of Cagliari, Cagliari, Italy
[4]Research and Technology Institute b<>com, 35510 Cesson-Sévigné, France
[5]Institute of Micromechanics and Photonics, Warsaw University of Technology, 02-525 Warsaw, Poland
*tobias.birnbaum@vub.be

Received 14 December 2022; revised 23 February 2023; accepted 23 February 2023; posted 24 February 2023; published 21 March 2023

Digital reconstructions of numerical holograms enable data visualization and serve a multitude of purposes ranging from microscopy to holographic displays. Over the years, many pipelines have been developed for specific hologram types. Within the standardization effort of JPEG Pleno holography, an open-source MATLAB toolbox was developed that reflects the best current consensus. It can process Fresnel, angular spectrum, and Fourier–Fresnel holograms with one or more color channels; it also allows for diffraction-limited numerical reconstructions. The latter provides a way to reconstruct holograms at their intrinsic physical instead of an arbitrarily chosen numerical resolution. The Numerical Reconstruction Software for Holograms v10 supports all large public data sets featured by UBI, BCOM, ETRI, and ETRO, in their native and vertical off-axis binary forms. Through the release of this software, we hope to improve the reproducibility of research, thus enabling consistent comparison of data between research groups and the quality of specific numerical reconstructions.

https://doi.org/10.1364/AO.483357

1. INTRODUCTION

Holography has made possible the (indirect) capture and replay of amplitude and phase information of visible light. When holography became digitally accessible through computer generation on more powerful computers, better camera sensors, and spatial light modulators, the field of digital holography (DH) came into existence.

Quickly the need arose to numerically propagate holograms efficiently. The diffraction and propagation of electromagnetic waves are governed by Maxwell's partial differential equations, which can be simplified to the scalar Rayleigh–Sommerfeld diffraction theory under several assumptions [1]. The scalar approximation has enormous practical significance because it correlates with the observed measurements in most real-world applications and provides computational simplifications. Nowadays, several computational methods are available for the numerical propagation of a digital hologram (abbreviated as well as DH) between planes.

While numerical propagation of DHs can be used in many parts of the holographic signal processing pipeline [2], the numerical reconstruction of DHs meant for visualization is of considerable interest. When observed from selected viewpoints, numerical reconstructions can provide a visual impression of the holographic content. The interest is high because the evaluation in a holographic display is time-consuming and affected by imperfections in the optical components. Thus, a fast but provisional method for quality assessment of DHs is the numerical reconstruction with subsequent viewing on alternative displays, such as conventional 2D or light-field displays [3]. By sequentially displaying an extensive range of 2D views extracted from a single hologram, the 3D scene exploration and experience can be approximated. With this quality assessment technique, several holographic signal processing algorithms can be evaluated, e.g., data compression schemes, pre-/post-processing steps, new deep neural-network topologies adapted to holography [4–6], hologram segmentation [7], motion compensation [8–11], or computer-generation algorithms [12–14].

Over the years, multiple software packages have been proposed that implement a subset of propagation models and their

own set of pre- and post-processing steps. Within the holographic signal processing community, each research group has its own numerical reconstruction steps. There are a few publicly available codebases [15–17], which have not found widespread adoption because they emphasize high computational performance while being limited in some sense, such as limited contribution rights, missing interface and documentation translation from non-English, or because they lacked functionality such as the accepted datatype, supported propagation methods, insufficient control over the post-processing steps, etc. Other commercial examples, such as [18], consider only digital-holographic microscopy applications.

The JPEG Pleno standardization effort by the ISO/JPEG body intends to release a new compression standard suitable for various kinds of static plenoptic imaging content, such as light fields, point clouds, and digital holograms [12,19]. The activities of the standardization effort on Part 5, JPEG Pleno holography, include(d) assembly of a versatile public JPEG Pleno database for DHs [20]; distillation of common test conditions, including a subjective and objective quality assessment pipeline [14,21]; and the development of a verification model [22,23].

As part of the quality assessment pipeline, the Numerical Reconstruction Software for Digital Holograms (NRSH) was developed in MATLAB. This software allows for extracting views from any DH in the JPEG Pleno database with little effort and focuses on accurate reconstruction and compatibility. Additionally, the software can also serve as a framework to modify and exchange hologram content for research and standardization. In [24], the authors provided a general overview of the design choices of the NRSH package v9 most relevant for quality assessment procedures. In this paper, we add a discussion on the fundamental properties of views reconstructed with orthographic or diffraction-limited perspective reconstructions, as implemented in NRSH. We also provide an updated overview of NRSH v10.

The paper is structured as follows: in Section 2, we provide a brief recap of the updated signal processing pipeline for NRSH v10. In Section 3, we compare numerical reconstructions from DHs using the new orthographic camera model versus the perspective camera model. We continue with a special case of perspective reconstructions, supported by NRSH, and discuss details on the logic of diffraction-limited perspective reconstruction in Section 4 using the concept of phase space. Finally, we conclude in Section 5.

2. NRSH: FUNCTIONAL OVERVIEW

NRSH ensures faithfulness of the reconstructions and complex-wavefield propagation according to best practices in visual quality assessment by JPEG Pleno holography, and it currently supports multiple propagation types such as the interim propagation of complex-valued wavefields, the reconstruction of extremely large DHs [25] (tens of giga-pixel), and the reconstruction of static images or video tours extracted from a single static DH. It implements the following three propagation kernels: single-Fourier-transform Fresnel propagation; propagation of Fourier-Fresnel holograms, as explained, e.g., here [26]; and the angular spectrum method [1].

In NRSH v10, the latter three propagation kernels were simplified and have an increased code similarity. The use and amount of interim zero-padding and coordinate systems were made more uniform. Furthermore, NRSH now supports, in addition to the perspective camera model, the orthographic mode. The software can be freely downloaded on the JPEG Pleno website [27]. Next, we highlight the current use cases of the NRSH package within JPEG Pleno holography before closing the section with a structural overview.

A. Quality Assessment

The NRSH software was already used to facilitate quality assessment experiments in [13,14,28]. Most important for the quality assessment was to ensure good control over the dynamic range of the reconstructions, and its reduction to a given integer bit-depth supported by the 2D assessment displays. For subjective quality assessment, the diffraction-limited perspective reconstruction was key to reducing the resolution to a displayable scale without potentially hiding compression artifacts.

Dynamic video tours were evaluated in [13]. Still, they were not adopted in the current common test conditions because of (1) informational overload causing the hiding of visual artifacts; (2) the high computational complexity; and (3) insufficient available scene complexity for prolonged 3D explorations.

B. Compression

In addition to quality assessment, the NRSH package can also be used with its "invertible" full-field propagation of complex-valued wavefields to facilitate the object plane compression of the classic image/video codecs. Namely, JPEG 2000 and H.265/HEVC, which are defined in the common test conditions document as anchor codecs for the nonbinary lossy compression pipeline, are also evaluated for compression performance in the object plane. The interim propagation of holograms to an in-focus object plane can improve the compression performance of traditional image compression techniques. This works best for holograms with a singular, shallow object as the object plane propagation concentrates the intensity of the wavefield to a well-defined region that resembles natural imagery. Note the interim full-field propagation to and from the object plane was specified to be implemented without zero-padding precisely because of its reversibility in the ideal case of lossless compression.

C. NRSH Structure

For nonmicroscopic DHs, the NRSH package proceeds as shown in Fig. 1. Provided some input hologram and a settings object, off-axis holograms are first converted into on-axis holograms in order to facilitate a homogeneous propagation and potential view reconstruction. Next, if either only complex-wavefield propagation or orthographic or full-field reconstructions are requested, the respective propagation kernels are called directly. Otherwise, a test for enabling the diffraction-limited reconstruction (DLR) with perspective follows. If DLR is enabled, a spatial aperture size is either parsed from the input settings or calculated based on a target resolution. Next, the spatial aperture is applied to the hologram using

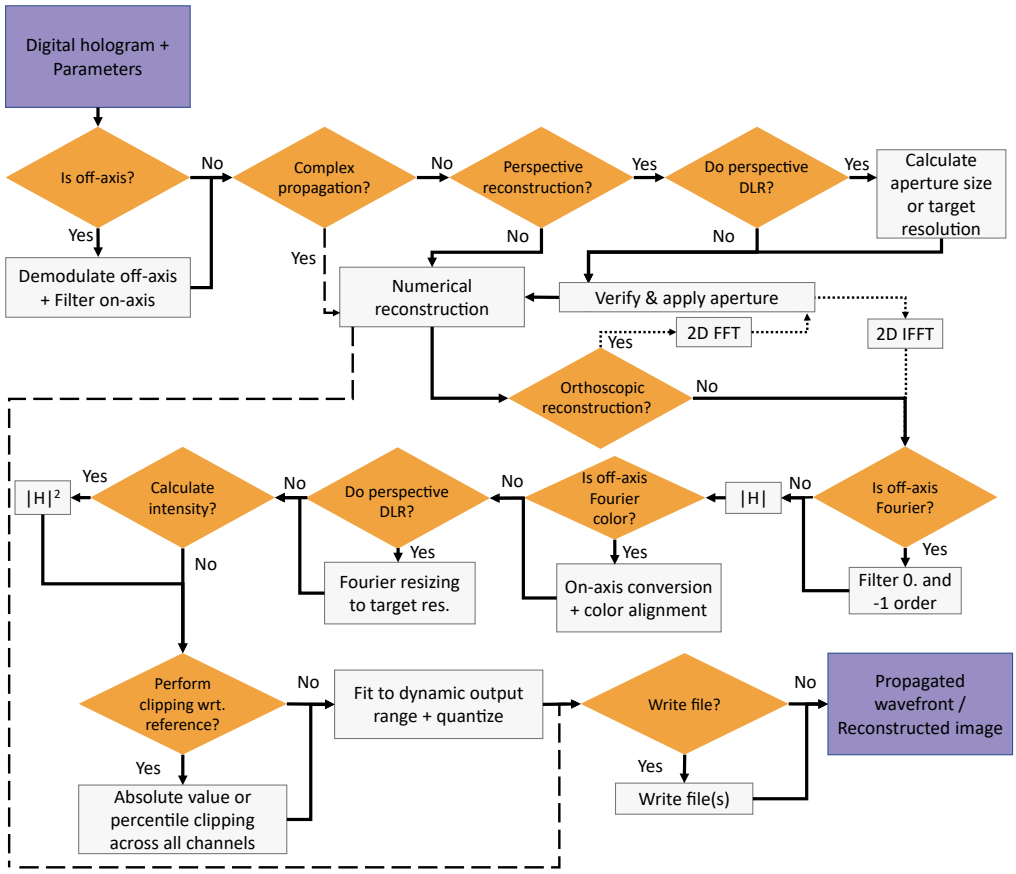

Fig. 1. Workflow of the NRSH package v10 for nonmicroscopic DHs from the JPEG Pleno database. DLR, diffraction limited reconstruction; FFT, fast Fourier transform.

a 2D Hann window to reduce ringing artifacts. Perspective reconstructions proceed with a numerical propagation.

For any propagation mode, but for the reconstruction of extremely large DHs, zero padding can be enabled to avoid aliasing impairing the reconstruction quality. While the complex-wavefield propagation terminates directly either by writing the result to a file or returning it directly, all other modes involve several more steps. In the case of orthographic reconstructions, the windowed aperture is applied in the Fourier domain post-propagation. Any propagation continues from here for non-Fourier holograms with the nonlinear operation of taking the absolute value of the complex-valued wavefield. Otherwise, uninteresting propagation orders are filtered first, and color channels are aligned after taking the absolute value. For perspective reconstructions with enabled DLR, a sinc-function-based resizing to the diffraction-limited resolution follows (see the discussion in Section 4). The pipeline terminates with an optional calculation of intensity, clipping, and quantization into 8 or 16 bit images.

The sequence of these steps ensures that the reconstructions for any two holograms that are similar but have experienced different processing (e.g., different compression levels) are comparable. In the following sections, we highlight two of NRSHs' core features and their characteristic impacts on the reconstruction quality. Specifically, we discuss view-specific reconstructions next and diffraction-limited perspective reconstructions thereafter.

3. VIEW-SPECIFIC RECONSTRUCTION

This section discusses the new functionality of orthographic reconstruction and how this differs from a perspective reconstruction of a DH. The orthographic and perspective camera models are widely used in computer graphics. An orthographic camera projects from the scene with collimated rays [see Fig. 2(a)]. In contrast, a perspective camera has a frustum with a nonzero opening angle [see Fig. 2(b)].

We will limit the discussion to near-field holograms. The discussion can be extended to Fourier holograms after one initial Fourier transform. The discussion also carries over to image-plane holograms directly for orthographic reconstructions, while some defocused interim plane needs to be chosen for perspective reconstructions.

Both reconstruction types can be implemented for a standard near-field hologram as follows. The numerical orthographic reconstruction of a DH is obtained by backpropagating the full hologram at a distance z and applying a limiting aperture in the Fourier domain wrt. the lateral spatial dimensions of the propagated field, cf. Fig. 3(a). The former operation selects a focus depth, while the latter selects all light corresponding to a given directionality. This can be understood through the equivalence

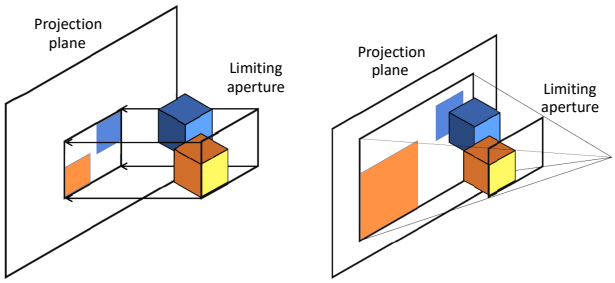

Fig. 2. Comparison of orthographic and perspective camera models in computer graphics and the perspective distortion. (a) Orthographic camera. (b) Perspective camera.

of spatial frequencies and viewing angles, as given by the grating equation

$$\sin(\Theta) = \lambda f_n \quad \text{with} \quad f_n = \frac{n}{Np} \quad \text{and}$$
$$n \in \left\{ \frac{-N}{2} + 1, \ldots, \frac{N}{2} \right\}, \tag{1}$$

with wavelength λ, diffraction angle Θ, spatial frequency f_n, and pixel pitch p. Therefore, an orthographic reconstruction selects viewing angles and samples, i.e., parts of the Fourier spectrum of the propagated DH.

In contrast, the most common way to obtain a perspective reconstruction from a DH is to apply a limiting aperture in the spatial domain of the original hologram (or another defocused plane) before computing its propagation by $z = z_{\text{obj}}$. This is illustrated in Fig. 3(b). While it is also conceptually possible to use a virtual lens function for viewpoint selection prior to propagation, this does not affect the discussion below in any way.

To understand the effects of either modality on the numerical reconstructions, we can use the well-known fact that the spatial size of the numerical aperture of an imaging system is roughly inversely proportional to the field of focus, i.e., the scene range that appears in focus. In the extreme case of a pinhole camera, everything is in focus. With this fact in mind, and knowing that only reconstructions with the perspective view model restrict the limiting spatial aperture of the system further than the hologram alone, we can explain the following key differences:

Depth of field. The orthographic reconstruction does not restrict the spatially limiting aperture of the DH in any way. Therefore, the hologram's depth of field is preserved. However, since perspective reconstruction introduces a spatially (more) limiting aperture a, the depth of field in the reconstruction is enlarged and varies approximately as $(a^{-1} - ax)^{-1}$ for some constant x. See also Fig. 4(g) versus Fig. 4(h) for a scene of depth 32.8 cm.

Speckle grain size. For the same reason, the lateral speckle grain size of the perspective reconstruction is larger than in the orthographic reconstruction. The lateral speckle resolution varies as $\sim D^{-2}$ [29], with D being the diameter of the holographic aperture [see also Fig. 4(g) versus Fig. 4(h)].

Intensity variance on position. As the orthographic reconstruction applies windowing to the spectrum of a DH, which is almost always nonuniform, the intensity of the reconstruction is viewpoint dependent. It is strongest for the center view and decreases toward the boundaries. For perspective reconstructions, there is no or almost no variance of intensity provided that the hologram plane is sufficiently distant, such that the entire scene can be reconstructed from the spatial subset of the hologram selected by the spatial limiting aperture. If the hologram plane is too close to the scene, then vignetting may occur because the information from some parts of the scene will not contribute into the selected aperture. For the intensity variations, see Figs. 4(a)–4(f).

Geometric deformation. Reconstructions obtained with a perspective reconstruction will naturally experience perspective distortion, as opposed to orthographic reconstructions. However, the difference will only be visually significant for deep scenes [see, for example, Figs. 4(g) and 4(h) versus Figs. 4(i) and 4(j)].

Given these differences, it depends on the objective of whether a less speckly reconstruction with a smaller depth of field, i.e., an orthographic or a perspective reconstruction, is more desirable for visualization. Furthermore, in practice, when using the angular-spectrum method for reconstructions, the orthographic model can be computationally more efficient than a perspective model, as only one propagation step is required for all views, and each additional view comes only at the cost of a single fast Fourier transform in the former case. In the perspective camera model, however, full propagation is required each time, and the issue may arise where an additional propagation to an interim out-of-focus plane is needed.

Ultimately, it is up to the user and the usage scenario to decide which reconstruction is more suitable. Within the scope of JPEG Pleno holography, thus far, only perspective reconstructions are used. These reconstructions better approximate human eye properties and allow for the computation

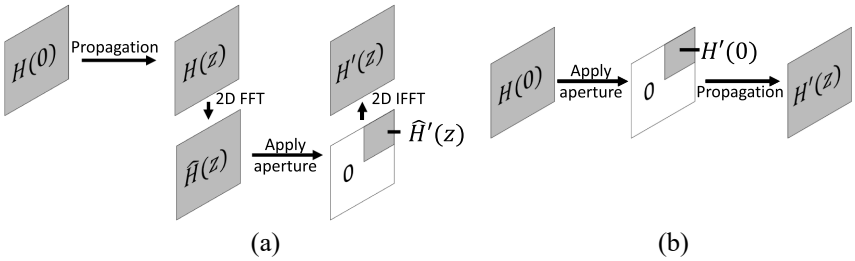

Fig. 3. Orthographic and perspective reconstructions from a hologram plane $z = 0$ to z. (a) Orthographic DH reconstruction. (b) Perspective DH reconstruction.

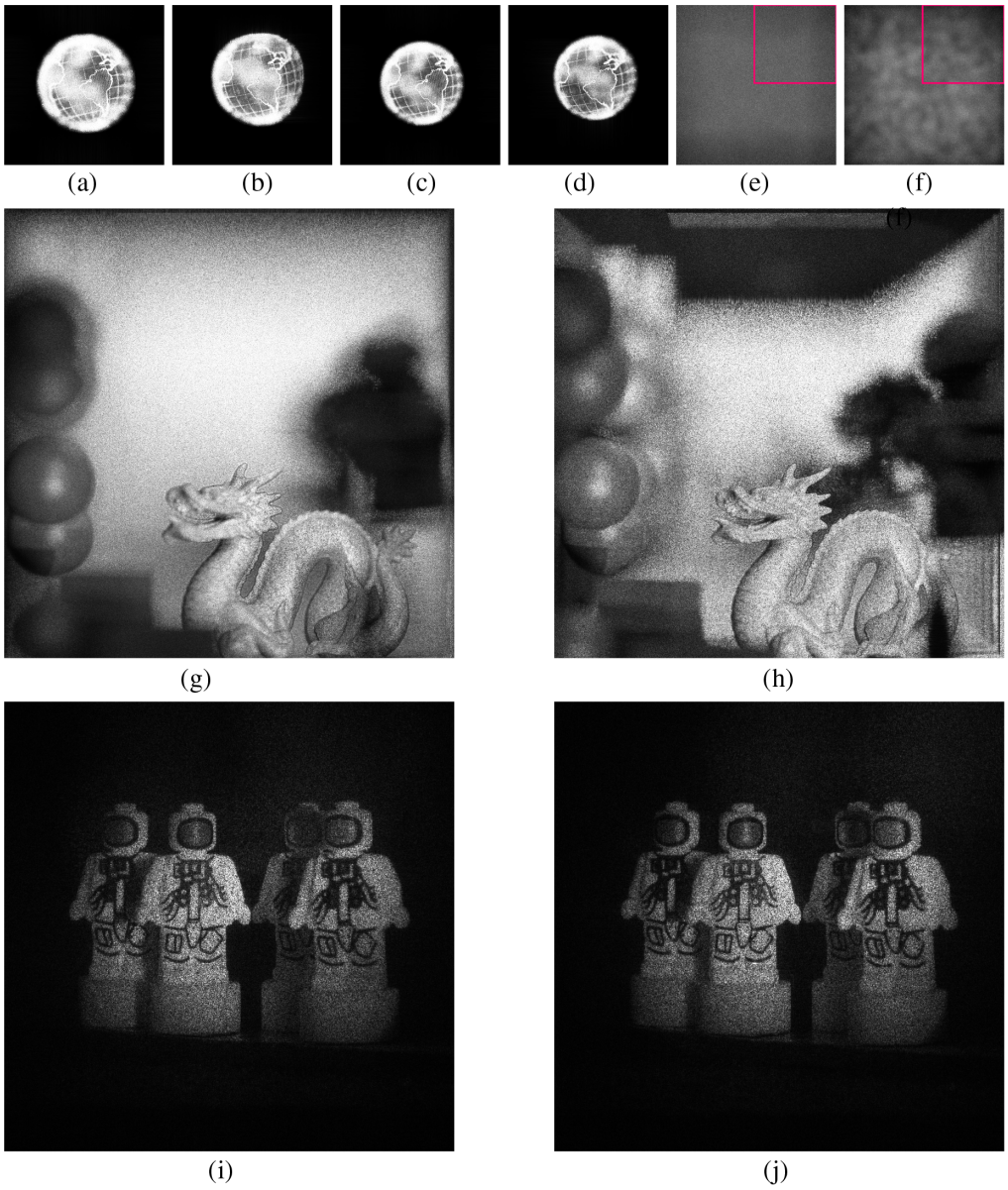

Fig. 4. Orthographic (a)–(b) versus perspective (c)–(d) distortion on "Diffuse Earth8K." Also visible is the lower intensity in corner views for orthographic reconstructions [see (b) versus (a)]. This is not the case for perspective reconstructions. Apertures applied to the hologram and Fourier domains are highlighted red in (e)–(f). (g) versus (h) The perspective distortions for a deep scene, the larger field of focus, and a larger speckle grain size in the latter, due to the smaller effective spatial aperture. In contrast, (i) versus (j) shows that there are no noticeable perspective distortions for shallow scenes.

of diffraction-limited reconstructions with subhologram resolutions.

4. DIFFRACTION-LIMITED PERSPECTIVE RECONSTRUCTION

As mentioned, the resolution of the perspective reconstruction from a DH with a resolution of $N_\xi \times N_\eta$ px results in an image of the same resolution. Upon visualization of numerically reconstructed DH on a regular 2D screen with an insufficient resolution, strategies for dimensionality reduction need to be investigated.

Downsampling without any relation to the actual information content of a given DH may easily hide artifacts that are supposed to be evaluated. The extraction of multiple regions of interest is unsuitable, as it amplifies the importance of speckle noise and usually leads to a complete loss of 3D perception. The conversion to pseudo-sequences was, for the moment, not deemed suitable for quality assessment of DHs for the reasons explained in Section 2.A.

The lateral resolution of a diffraction-based imaging system is limited either by diffraction (i.e., the maximal available bandwidth provided an illumination wavelength of λ) or by the available (spatial) bandwidth. The band limitation of a discretized system can be attributed to (a) the finite sampling pitch

(which is inversely proportional to half the maximum sampling frequency of a complex-valued signal), and (b) the finite extent of the DH as well as its position relative to the object because PSFs have a spatially varying frequency spectrum. As shown in the former section, since almost every perspective numerical reconstruction is band-limited through at least a limiting spatial aperture, the authors implemented a method in NRSH to calculate the diffraction-limited reconstruction of any perspective reconstruction of a DH. The *ab initio* method utilizes solely general system characteristics such as aperture size and position, object distance, hologram resolution, wavelength, and pixel pitch. Note that this approach may only influence the chosen aperture size or perform a Fourier resizing of the obtained high-resolution image. No manipulation of the underlying hologram is performed. This approach was only briefly discussed in [30].

Conceptually, the problem statement is depicted in an exaggerated way in Fig. 5 for the case of a limiting aperture with pixel pitch $p > \frac{\lambda}{2}$. In this section, we will explain the derivation of the method.

Without loss of generality, we consider the following general defocused holograms and rigorous propagation implemented, for example, via the angular spectrum method. However, for simplicity, we will assume the separability of the spatial frequency components and use only one spatial dimension.

The ansatz is based on phase-space methods [31], which consider spatial frequencies and spatial components within a DH simultaneously. Consider the 2D phase space along a 1D cross-section of an arbitrary complex-valued DH. Indeed, its signal bandwidth is contained within the light blue contour shown in Fig. 6(a). Tracking the footprint of any spatial aperture (for perspective reconstruction) of A_ξ pixel shown in dark blue upon propagation will shear the selection of all frequencies within the spatial aperture in Fig. 6(a) into the sigmoidal shape shown in Fig. 6(b). It is essential to realize that the effective bandwidth is still given as the difference of the highest and lowest spatial frequencies for any position $x \in x_a \pm \frac{a}{2}$ within the aperture.

Using the principle of stationary phase and the expression of instantaneous frequency for the rigorous propagation kernel from [30], the spatial frequency along ξ is given for a 1D DH as

$$f_\xi := \frac{1}{2\pi}\frac{\partial \phi}{\partial \xi} = -\frac{(\xi - x)}{\lambda\sqrt{(x-\xi)^2 + z^2}}. \tag{2}$$

With this and $\xi = x_a \pm \frac{a}{2}$, we can immediately derive the following two expressions for the upper and lower spatial frequency boundaries of a propagated spatial aperture as

$$f_x^{\mathrm{up}}(x) := \frac{x - \left(x_a + \frac{a}{2}\right)}{\lambda\sqrt{\left(x - \left(x_a + \frac{a}{2}\right)\right)^2 + z_{\mathrm{rec}}^2}} \quad \text{and}$$

$$f_x^{\mathrm{down}}(x) := \frac{x - \left(x_a - \frac{a}{2}\right)}{\lambda\sqrt{\left(x - \left(x_a - \frac{a}{2}\right)\right)^2 + z_{\mathrm{rec}}^2}}. \tag{3}$$

From this, the absolute effective bandwidth τ of the complex wavefield anywhere within the aperture is given as

$$\tau(x) := \min\left(\left|f_x^{\mathrm{up}}(x) - f_x^{\mathrm{down}}(x)\right|, 2f_B\right). \tag{4}$$

Thereby, the maximal spatial frequency f_B physically supported by the hologram is given as

$$f_B := \min\left(\frac{1}{p}, \frac{1}{\lambda}\right), \tag{5}$$

unless chosen smaller on purpose.

The effective bandwidth is largest in the center of the propagated aperture and falls off symmetrically toward its borders, unless the spatial extent of the hologram itself is gating it further. The maximal bandwidth of the complex-valued wavefield of the propagated aperture can thus be estimated as

$$\tau \approx \min\left(\frac{a}{\lambda\sqrt{\frac{a^2}{4} + z_{\mathrm{rec}}^2}}, 2f_B\right). \tag{6}$$

The next step of any numerical reconstruction involves the application of the absolute value. Without the use of any specific signal model, it can only be said that the bandwidth at most doubles. Putting everything together, the diffraction-limited resolution N_ξ^{eff} of the absolute part of a propagated aperture is at most

$$N_\xi^{\mathrm{eff}} := 2pN_\xi\tau. \tag{7}$$

Resizing any numerical reconstruction in Fourier space (due to the constraints being posed on the signal bandwidth) to this resolution guarantees that no information, which would be visible in an ideal optical setup, is lost. Because the fast Fourier transforms used for this operation assumes periodicity of the signal, it is recommended to apodize in Fourier space using, for example, a Hann window, although empirically this was never required for the holograms contained in the JPEG pleno database due to their spectral intensity profile.

The effects of the resizing are drastic, and the reconstruction from b<>com's "Dices16K" hologram using an aperture of size 2048 × 2048 results in a reconstruction that is about 10.34%

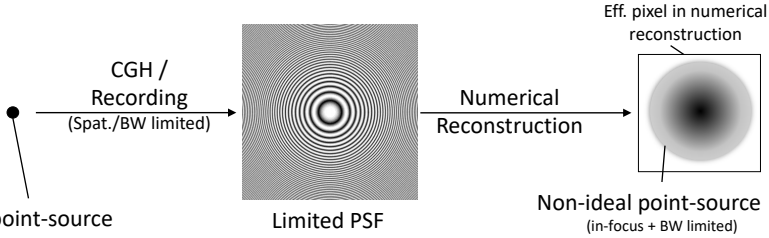

Fig. 5. Problem model for the effect of bandwidth limitation on the numerical resolution of perspective reconstructions from DH.

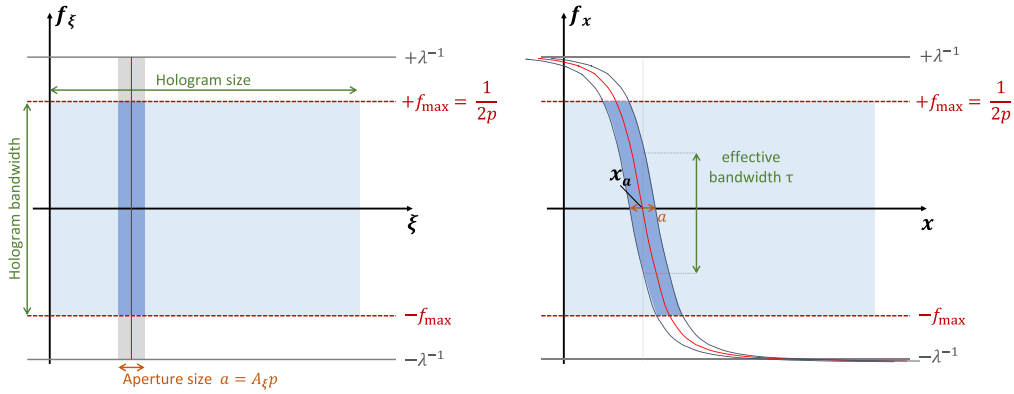

(a) (b)

Fig. 6. Phase space modeling of the space-bandwidth product of an arbitrary DH (light blue) with applied aperture (dark blue) in (a) the hologram plane at $z = 0$ and (b) in the image/object plane after propagation to z_{rec}.

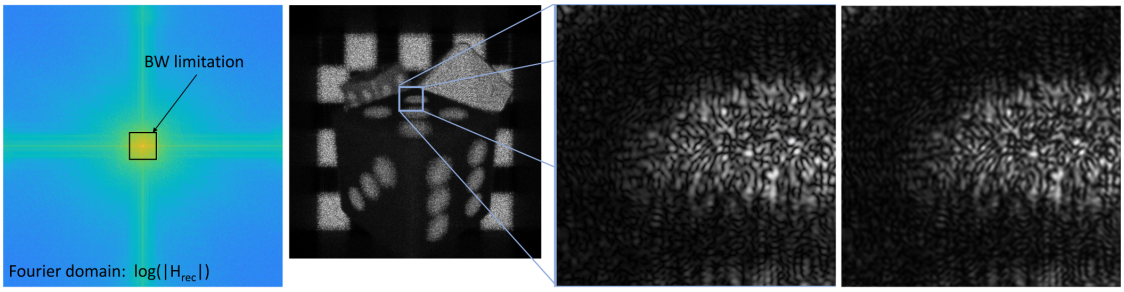

(a) (b) Native resolution ROI (1024 × 1024 px) (c) Proposed ROI (105 × 105 px)

Fig. 7. (a) Low-pass filtering in the Fourier domain of the reconstructed high-resolution wave field amplitude, where vital information is located only within the proposed BW limitation. (b) High-resolution reconstruction, downsampled for visualization, and ground-truth ROI selection are shown. (c) Same ROI after proposed low-pass filtering in the Fourier domain.

of the size of the hologram. Figure 7 shows an explicit example of the Fourier footprint of the reconstruction amplitude, the cropped effective bandwidth, and zoomed regions from the reconstruction at the native and the proposed resolution.

Naturally, Eq. (7) can be used either to compute the effective resolution from a given aperture and hologram size, or it can be used to deduce an aperture size provided a target resolution. Both modes are implemented and supported in the NRSH v10 package.

5. CONCLUSION

In this paper, we provided an update on the signal processing pipeline implemented in the NRSH v10 package. We then discussed the effects of specific reconstruction mode choices, namely, the orthographic, perspective, and diffraction-limited perspective reconstructions. We have seen that orthographic and perspective reconstructions potentially differ noticeably, depending on in which domain a limiting aperture is applied; either choice has benefits and drawbacks. Thereafter, we discussed how *ab initio* estimates could provide an upper bound for the diffraction-limited resolution of any numerical perspective reconstruction from a hologram and showed examples as used in the JPEG Pleno holography efforts.

Although the NRSH package was initially only developed for the purpose of providing a well-defined reconstruction toolbox for quality assessment with JPEG Pleno holography, it has slowly matured into a feature-rich, publicly available MATLAB toolbox for the reconstruction of a large variety of DHs. We hope that its design and code base will inspire further research in the field of DH and improve the comparability and reproducibility of scientific results.

Funding. Fonds Wetenschappelijk Onderzoek (12ZQ220N, 12ZQ223N); National Research Agenc (ANR-A0-AIRT-07); Narodowe Centrum Nauki (UMO-2018/31/B/ST7/02980).

Acknowledgment. This research was funded by the Research Foundation, Flanders (FWO), and by the French government through the National Research Agency (ANR) Investment referenced and through Narodowe Centrum Nauki.

Disclosures. The authors declare no conflicts of interest.

Data availability. Data underlying the results presented in this paper are available in [20].

REFERENCES

1. J. W. Goodman, *Introduction to Fourier Optics*, 4th ed. (W. H. Freeman, 2017).
2. D. Blinder, A. Ahar, S. Bettens, T. Birnbaum, A. Symeonidou, H. Ottevaere, C. Schretter, and P. Schelkens, "Signal processing

challenges for digital holographic video display systems," Signal Process. Image Commun. **70**, 114–130 (2019).
3. A. Ahar, M. Chlipala, T. Birnbaum, W. Zaperty, A. Symeonidou, T. Kozacki, M. Kujawinska, and P. Schelkens, "Suitability analysis of holographic vs light field and 2D displays for subjective quality assessment of Fourier holograms," Opt. Express **28**, 37069–37091 (2020).
4. T. Shimobaba, D. Blinder, T. Birnbaum, I. Hoshi, H. Shiomi, P. Schelkens, and T. Ito, "Deep-learning computational holography: a review," Front. Photon. **3**, 854391 (2022).
5. L. Shi, B. Li, C. Kim, P. Kellnhofer, and W. Matusik, "Towards real-time photorealistic 3D holography with deep neural networks," Nature **591**, 234–239 (2021).
6. Y. Rivenson, Y. Wu, and A. Ozcan, "Deep learning in holography and coherent imaging," Light Sci. Appl. **8**, 85 (2019).
7. T. Birnbaum, D. Blinder, R. K. Muhamad, C. Schretter, A. Symeonidou, and P. Schelkens, "Object-based digital hologram segmentation and motion compensation," Opt. Express **28**, 11861–11882 (2020).
8. D. Blinder, C. Schretter, and P. Schelkens, "Global motion compensation for compressing holographic videos," Opt. Express **26**, 25524–25533 (2018).
9. R. K. Muhamad, D. Blinder, A. Symeonidou, T. Birnbaum, O. Watanabe, C. Schretter, and P. Schelkens, "Exact global motion compensation for holographic video compression," Appl. Opt. **58**, G204–G217 (2019).
10. H. Cao, "Speckle-based spectrometers," in *Digital Holography and Three-Dimensional Imaging* (Optical Society of America, 2019), paper Th1B.1.
11. T. Shimobaba, S. Katsuyama, T. Nishitsuji, I. Hoshi, H. Shiomi, F. Wang, T. Kakue, N. Takada, and T. Ito, "Motion parallax holograms generated from an existing hologram," Appl. Sci. **11**, 2933 (2021).
12. R. K. Muhamad, T. Birnbaum, A. Gilles, S. Mahmoudpour, K.-J. Oh, M. Pereira, C. Perra, A. Pinheiro, and P. Schelkens, "JPEG Pleno holography: scope and technology validation procedures," Appl. Opt. **60**, 641–651 (2021).
13. A. Ahar, M. Pereira, T. Birnbaum, A. Pinheiro, and P. Schelkens, "Validation of dynamic subjective quality assessment methodology for holographic coding solutions," in *13th International Conference on Quality of Multimedia Experience (QoMEX)* (2021), pp. 7–12.
14. A. M. G. Pinheiro, J. Prazeres, A. Gilles, R. K. Muhamad, T. Birnbaum, and P. Schelkens, "Definition of common test conditions for the new JPEG Pleno holography standard," Proc. SPIE **12138**, 121380N (2022).
15. M. Jing, F. Yanfang, and T. Penghui, "Research on digital holographic 3D reconstruction software," in *2nd International Conference of Sensor Network and Computer Engineering (ICSNCE)* (Atlantis, 2018), pp. 105–108.
16. J. Hong, Y. Kim, H. Bae, and S. Hong, "Openholo: open source library for hologram generation, reconstruction and signal processing," in *Imaging and Applied Optics Congress* (Optical Society of America, 2020), paper HF3G.1.
17. T. Shimobaba, J. Weng, T. Sakurai, N. Okada, T. Nishitsuji, N. Takada, A. Shiraki, N. Masuda, and T. Ito, "Computational wave optics library for C++: CWO++ library," Comput. Phys. Commun. **183**, 1124–1138 (2012).
18. M. M. Mansoor, J. D. Trolinger, and J. George, "A versatile digital holography software for three-dimensional investigations," Proc. SPIE **11817**, 118170B (2021).
19. P. Schelkens, Z. Y. Alpaslan, T. Ebrahimi, K.-J. Oh, F. M. B. Pereira, A. M. G. Pinheiro, I. Tabus, and Z. Chen, "JPEG Pleno: a standard framework for representing and signaling plenoptic modalities," Proc. SPIE **10752**, 107521P (2018).
20. https://jpeg.org/jpegpleno/plenodb.html, 2022.
21. "JPEG Pleno Holography Common Test Conditions 5.0," (2021).
22. R. K. Muhamad, T. Birnbaum, D. Blinder, C. Schretter, and P. Schelkens, "INTERFERE: a unified compression framework for digital holography," in *Digital Holography and Three-Dimensional Imaging* (Optica, 2022).
23. R. K. Muhamad, T. Birnbaum, D. Blinder, and P. Schelkens, "INTERFERE, short-time Fourier transform based compression of complex-valued holograms with bit-depth and range-adaptive quantization," IEEE Trans., submitted for publication.
24. T. Birnbaum, D. Blinder, R. K. Muhamad, A. Gilles, C. Perra, T. Kozacki, and P. Schelkens, "A standard way for computing numerical reconstructions of digital holograms," Proc. SPIE **12138**, 121380O (2022).
25. A. Gilles and P. Gioia, "Compression and reconstruction of extremely-high resolution holograms based on hologram-lightfield transforms," Proc. SPIE **11510**, 1151006 (2020).
26. T. Kozacki, M. Chlipala, and P. L. Makowski, "Color Fourier orthoscopic holography with laser capture and an LED display," Opt. Express **26**, 12144–12158 (2018).
27. https://ds.jpeg.org/documents/jpegpleno/wg1n100342-097-PCQ-Numerical_Reconstruction_Software_for_Holography_v10_0.zip, 2022.
28. J. Prazeres, R. K. Muhammad, T. Birnbaum, A. Gilles, P. Schelkens, and A. M. G. Pinheiro, "Quality evaluation of the JPEG Pleno holography call for proposals response," in *QoMEX* (2022).
29. J. W. Goodman, *Speckle Phenomena in Optics: Theory and Applications* (Roberts & Company, 2010).
30. T. Birnbaum, D. Blinder, and P. Schelkens, "Diffraction limited perspective, numerical reconstruction of macroscopic DH," in *OSA Imaging and Applied Optics Congress 2021 (3D, COSI, DH, ISA, pcAOP)* (OSA, 2021).
31. T. Birnbaum, T. Kozacki, and P. Schelkens, "Providing a visual understanding of holography through phase space representations," Appl. Sci. **10**, 4766 (2020).